OPEN ACCESS
IOP Publishing | Songshan Lake Materials Laboratory
Materials Futures
Mater. Futures 2 (2023) 022701 (15pp)
https://doi.org/10.1088/2752-5724/accd87

Topical Review

In-materio reservoir computing based on nanowire networks: fundamental, progress, and perspective

Renrui Fang[1,3], Woyu Zhang[1,3], Kuan Ren[1], Peiwen Zhang[1], Xiaoxin Xu[1,3], Zhongrui Wang[2] and Dashan Shang[1,3,*]

[1] State Key Laboratory of Fabrication Technologies for Integrated Circuits, Institute of Microelectronics of Chinese Academy of Sciences, Beijing 100029, People's Republic of China
[2] Department of Electrical and Electronic Engineering, The University of Hong Kong, Hong Kong 999077, People's Republic of China
[3] University of Chinese Academy of Sciences, Beijing 100049, People's Republic of China

E-mail: shangdashan@ime.ac.cn

Received 7 March 2023, revised 29 March 2023
Accepted for publication 10 April 2023
Published 19 May 2023

Abstract

The reservoir computing (RC) system, known for its ability to seamlessly integrate memory and computing functions, is considered as a promising solution to meet the high demands for time and energy-efficient computing in the current big data landscape, compared with traditional silicon-based computing systems that have a noticeable disadvantage of separate storage and computation. This review focuses on in-materio RC based on nanowire networks (NWs) from the perspective of materials, extending to reservoir devices and applications. The common methods used in preparing nanowires-based reservoirs, including the synthesis of nanowires and the construction of networks, are firstly systematically summarized. The physical principles of memristive and memcapacitive junctions are then explained. Afterwards, the dynamic characteristics of nanowires-based reservoirs and their computing capability, as well as the neuromorphic applications of NWs-based RC systems in recognition, classification, and forecasting tasks, are explicated in detail. Lastly, the current challenges and future opportunities facing NWs-based RC are highlighted, aiming to provide guidance for further research.

Keywords: reservoir computing, nanowire networks, short-term memory, dynamic characteristics, neuromorphic computing

1. Introduction

In recent years, thanks to fast advances in neuroscience and neural network algorithms, the fast-growing artificial intelligence (AI) technology allows human society to enter into an era of intelligence through its successful application to a lot of fields such as the internet of things, medical diagnosis, intelligent robots, etc [1]. At present, online AI services are optimized through cloud computing. Specifically, the optimization is achieved using algorithms on computers to analyze and process big data from the edge of the internet to achieve target tasks. There is an exponentially growing number of data generated by intelligent edge devices. However, the existing computing system still relies on the traditional von Neumann

* Author to whom any correspondence should be addressed.

architecture with separated storage and computing units, resulting in a frequent data transfer brought by limited bandwidth of data path and leading to huge latency and energy consumption [2, 3]. Meanwhile, metal-oxide-semiconductor field effect transistors functioning as its basic component struggle to improve integration and performance by further reducing size as Moore's law slows down [4]. As a result, the existing computing system consumes more time and energy, making it difficult to meet the rapidly growing demand for development of an intelligent society.

In order to get rid of this dilemma, a potential answer is to employ novel devices to develop brain-inspired neuromorphic computing diagrams by simulating the functions of biological neural network which is comprised of $\sim 10^{11}$ neurons randomly connected by $\sim 10^{15}$ synapses and has plenty of superiorities especially in in-memory computing architecture and low power consumption (only 20 fJ per operation) [5–8]. As a kind of neuromorphic computing architecture, artificial neural networks which are usually divided into feedforward neural networks (FNNs) and recurrent neural networks (RNNs) receive numerous attentions. FNNs are mainly used to process static (time-independent) data. On the contrary, RNNs have cyclic connections in structure, so that its output state at a certain moment not only relates to the input signal at present moment but also to the past state, that is, it is equipped with a short-term memory ability and can be used to process time-dependent information. However, it is well-known that RNNs have drawbacks in training and hardware implementation. Thus, researchers begins to explore a new approach known as RC.

RC originating from RNNs is also suited for handling timing information, and attracts considerable attentions due to its unique advantages particularly in optimized training process. The research on RC is originated from echo state network (ESN) proposed by Jaeger in 2001 [9] and Liquid State Machine (LSM) proposed by Maass *et al* in 2002 [10]. The major difference between them is that the former usually uses the random network formed by large-scale sparsely connected Sigmoid neurons as the hidden layer, while the latter uses pulse neurons to construct hidden layer. However, both of them are essentially the same, for the fact of using a large number of neurons to form random and sparsely connected networks acting as the hidden layer, which is called 'reservoir', and utilizing its dynamic characteristics to deal with time series problems. Therefore, ESN and LSM are collectively called RC.

The conventional RC model (figure 1) which mainly includes three parts, i.e. input layer, reservoir, and output layer, can be described by the formula as follows:

$$x(t) = f(W_{\text{in}} \cdot u(t) + W_{\text{re}} \cdot x(t-1)) \tag{1}$$

$$y(t) = W_{\text{out}} \cdot x(t) \tag{2}$$

where $x(t)$ and f are the reservoir state at time t and the transforming function of a reservoir node respectively [11]. Notably, W_{in} and W_{re} are randomly generated and fixed, and need no training. Instead, only W_{out} requires tuning towards target signals using simple linear regression algorithm, which makes the training very efficient by breaking down to a simple matrix multiplication [12]. Compared with the conventional RNNs, this simple and fast training process can greatly reduce the computational energy and time consumption in the learning process, and also effectively avoid the problems of gradient disappearing and gradient explosion in the training process based on the gradient class learning algorithm [13]. Other than this traditional network-type RC, there are several other types of RC developed after years of research. For example, the delayed RC with a single real nonlinear node employing a delayed feedback loop based on time-multiplexing of input signals contributes to much easier implementation as only one physical node is required [14]. Moreover, the introduction of delayed feedback loop not only increases the computational power with a single node but also provides a way to characterize the properties of reservoir in degree of complexity through analyzing the delayed system potential to exhibit chaotic oscillations [104, 15]. But the use of virtual nodes instead of real nodes limits the dynamics and thus the computing abilities compared with the one with several real nonlinear nodes. Additionally, the deep RC based on spatial multiplexing is composed of multiple standard reservoir layers which are stacked one on top of each other, enriching its complex dynamics [16]. The deep layered organization enhances its hierarchical information processing ability and short-term memory capacity [17]. Apart from them, the next generation RC (NGRC) based on nonlinear vector autoregression (NVAR) and characterized by the absence of reservoir requires no random matrices, fewer metaparameters, and provides interpretable results with shorter training data sets and training time compared with other approaches [18, 19].

Hitherto, the hardware implementation of RC is mainly based on various physical phenomena in the real word. Physical RC systems per se have various changes, so there is no need for special training to adapt to the changes, that is, the W_{re} needs no training, thus greatly reducing the learning cost. Various physical devices and systems with nonlinear dynamics have been used to work as a computational resource relying on different mechanisms, such as memristors [20–23], transistors [24–27], spintronic oscillators [28], magnetic skyrmions [29], photonic systems [30, 31], and others [32–35], which increase the diversity of reservoir and results in the thriving development of physical RC. In this regard, we have realized a three-dimensional (3D) RC employing a 4-layer 3D vertical dynamic memristor array [36], and implemented an energy efficient RC system using ultrathin ferroelectric tunneling junctions with transient depolarization property for temporal signal processing in our previous works [37]. We also proposed a new hardware implementation way for the NGRC based on in-memory computing paradigm, in which the matrix vector multiplication during NVAR process is performed by memristor array, further improving the energy efficiency [38]. These studies further reveal the potential of RC in time-dependent information processing. Notably, the emergence of a lot of intelligent matters such as self-assembled nanowires further provides platforms and motivations to physically realize RC and perform computing in material

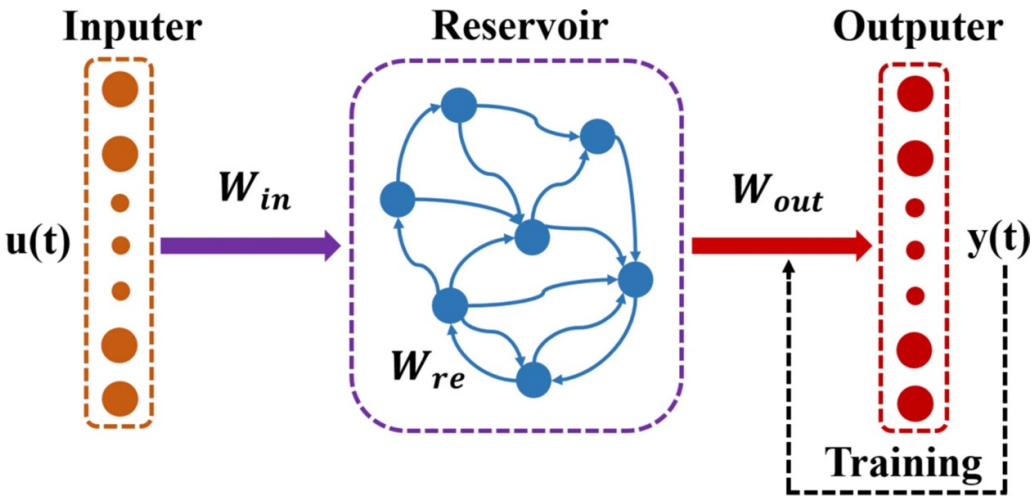

Figure 1. Schematic representation of RC paradigm. The reservoir with constant weights (W_{re}) is a RNN randomly connected by a lot of coupled nonlinear nodes, playing a role of mapping the input signal ($u(t)$) through input weights (W_{in}) into a higher dimensional feature space, and followed by the analysis of outputer via output weights (W_{out}) to produce output signals ($y(t)$).

(called in-materio RC) using the intrinsic properties of materials [39].

Among many physical systems, NWs-based RC receives growing attentions recently. For one thing, the self-organization confers NWs with high synaptic connectivity among the nodes and provides adaptability, fault tolerance and robustness, which induces a great similarity with respect to biological neural systems while of which the individual elements lack. For another, the self-organized systems emphasize the emergent dynamics of the whole system with no need for fine tuning constituent elements. These advantages make NWs appear as the most promising platform for in-materio implementation of brain-inspired RC [40]. Here, we concentrate on NWs-based RC and systematically review the recent progress from perspectives of device preparation, operation mechanism, dynamic characteristics, and neuromorphic applications, and summarize the current problems remaining to be tackled in the end.

2. Preparation of NWs-based reservoir

The preparation of NWs-based reservoir device can be conducted through chemical synthesis combined with traditional CMOS technology. The process is usually divided to three steps: the synthesis of nanowires, the fabrication of NWs, and the preparation of multi-electrode arrays.

2.1. Synthesis of nanowires

Nanowires coated by various functional materials are regarded as a kind of one-dimensional materials with core/shell structure. Depending on the materials used, nanowires are generally distinguished to three types. One is metal/metal-inorganic compound nanowire, such as Ag/Ag_2S, Ag/Ag_2Se, Ag/AgI, Ag/TiO_2, Ni/NiO, and Cu/CuO nanowires [41]. Another is metal/organic nanowire whose classical example is Ag/polyvinyl pyrrolidone (PVP) nanowire. And the other is organic/organic nanowire like the single-walled carbon nanotube (SWNT)/polyoxometalate (POM), SWNT/porphyrin-polyoxometalate (Por-POM) nanowire, and SWNT/liquid crystal [42]. Among these nanowires, Ag nanowires and POM-coated SWNT nanowires drawing extensive attentions are the current research hotpots, and the corresponding surface microstructures are shown in figures 2(a) and (b), respectively.

Nanowires can be synthesized in different ways depending on the materials used. The common synthesis methods include redox method, polyol method, ultrasonic dispersion method, and template method. Among them, Ag_2S, AgI and other inorganic compounds coated metal Ag nanowires are usually synthesized by redox method which is to deposit part of the copper column on the substrate at first, and then drop a certain amount of $AgNO_3$ solution. Since the chemical activity of Cu is greater than that of Ag, Cu can displace the Ag in $AgNO_3$ through spontaneous chemical reaction as shown in formula (3), giving rise to the generation of a lot of Ag nanoparticles which connect with each other to form randomly oriented Ag nanowires in solution [43]. The reaction as shown in formulas (5) and (6) would then occur by placing the Ag nanowires in suitable sulfur gas or iodine gas environment, making the surface Ag be vulcanized or iodized into Ag_2S [44] and AgI [43], respectively. At the same time, the Ag/Ag_2S/Ag and Ag/AgI/Ag metal–insulator-metal (MIM) interfaces are formed at the crossbar junction of the Ag nanowires. Differently, the Ag_2Se nanowires are formed by the redox reaction between α-Se nanowires and $AgNO_3$ solution under certain conditions as shown in formula (6) [45],

$$Cu_{(s)} + 2Ag^{+}_{(aq)} \rightarrow Cu^{2+}_{(aq)} + 2Ag_{(s)} \quad (3)$$

$$2Ag_{(s)} + S_{(g)} \rightarrow Ag_2S_{(s)} \quad (4)$$

$$2Ag_{(s)} + I_{2(g)} \rightarrow 2AgI_{(S)} \quad (5)$$

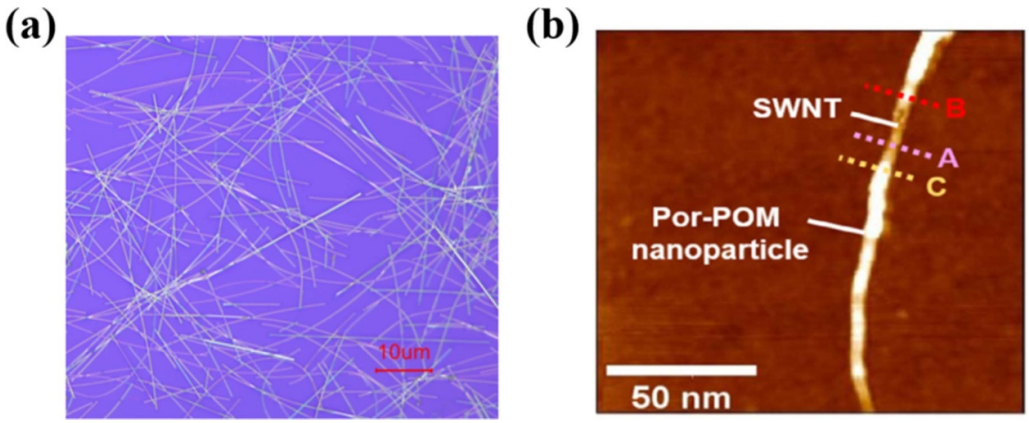

Figure 2. (a) Optical microscopy (OM) image of a highly interconnected memresistive NW (scale bar, 10 μm) which is prepared using Ag/PVP nanowires with a diameter of 120 nm and length of 20–50 nm and dynamic spinning coating process with a rotating speed of 1500 rpm. (b) Atomic force microscope (AFM) image with the height color bar of a single SWNT/Por–POM complex. Reproduced from [49]. CC BY 4.0.

$$3Se_{(s)} + 6Ag^{+}{}_{(aq)} + 3H_2O_{(aq)} \rightarrow 2Ag_2Se_{(s)} + Ag_2SeO_{3(s)} + 6H^{+}{}_{(aq)}. \quad (6)$$

As for Ag/PVP nanowires, the most commonly used synthesis method is polyol method, which is adding polyol as reducing agent in PVP to reduce Ag^+ in $AgNO_3$ to Ag, and dispersing in absolute ethyl alcohol to obtain nanowire solution [46, 47]. SWNT/POM nanowires are formed by ultrasonic dispersion of PMo_{12} and SWNT mixed solution, which makes PMo_{12} absorb on the surface of SWNT [48, 49].

2.2. Fabrication of NWs

The fabrication of NWs is mainly to get thin film with random cross interconnect network structure. For Ag nanowires coated with inorganic compounds, a randomly oriented dendritic complex network structure is formed accompanying with the redox reaction in the solution [50]. A thin film will be generated after the reaction by adjusting the amount of $AgNO_3$ added according to the size of the selected substrate. The corresponding preparation process is shown in figure 3(a). The prepared nanowire solution is dropped on the rotating substrate by dynamic spinning coating, and evenly coated on the substrate surface by centrifugal force. After a period of natural drying, the NW is obtained. In the process of spinning coating, the density of nanowire junction and the thickness of the film can be controlled by adjusting the content of the nanowire solution added by drops and the rotating speed of spin coating. Dissimilarly, the deposition method of SWNT/POM nanowire film is to filter its suspension solution after centrifugation using nitrocellulose filter paper, and then transfer the obtained film to the substrate [48].

2.3. Preparation of multi-electrode arrays

The preparation of multi-electrode arrays can be realized by traditional CMOS technology. For nanowires without organic matter such as Ag/Ag_2S nanowire, the designed array pattern is first transferred from mask to nanowires and substrate by lithography technology followed by electron beam evaporation or magnetron sputtering process to generate an inert metal film, and then the excess metal film is removed by lift-off process, so as to obtain the designed metal electrode. The specific process is shown in figure 3(b). Nevertheless, the nanowires containing organic matters such as Ag/PVP nanowire cannot achieve the graphic of electrode arrays by photolithography technology. The organic matters like photoresist, ethanol, and acetone used in the lithography process inevitably damage the PVP layer and the structure of nanowires due to the good compatibility of PVP with most organic matters. An alternative way is to adopt a shadow mask to implement the process, as shown in figure 3(c). That is, the designed electrode array pattern is transferred to a shadow mask through laser cutting, and then the substrate and mask are fixed together to conduct the electron beam evaporation or magnetron sputtering metal film process. The metal would be deposited onto the nanowires through holes in the mask, enabling the electrode array to be prepared as expected. The main purpose of electrode preparation is to arrange the electrode with a certain spacing, so as to fix the distance between the probes used in test. Hence, it is also possible to fix the distance between the probes by designing the probe platform externally without preparing the electrodes for test [51, 52], as shown in figure 3(d).

3. Working mechanism of nanowires

The MIM sandwich structure formed at the crossing junctions in the nanowires networks can be viewed as a two-terminal device. Resulting from different materials used, nanowires exhibit two different working mechanisms, namely memresistive and memcapacitive principles, which are caused by changes in resistance and capacitance respectively. In this regard, the memcapacitive NWs feature a higher energy efficiency compared to memresistive one when addressing identical complex tasks, for the reason that the memcapacitive element without consuming static energy is a capacitance in

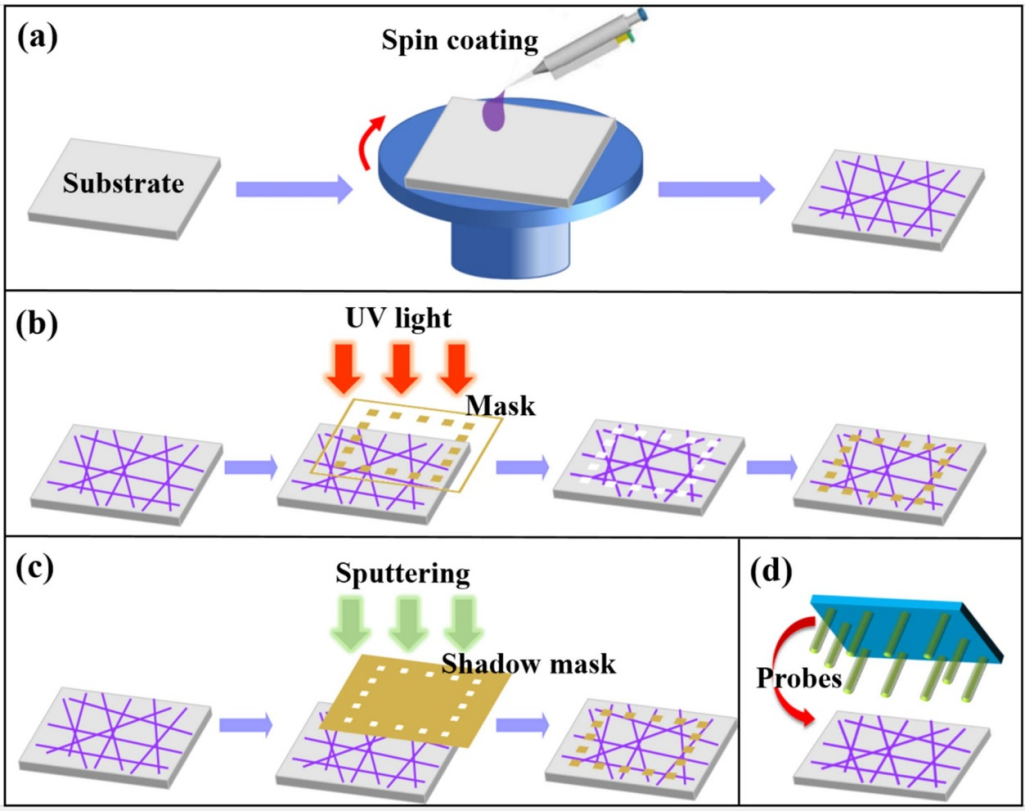

Figure 3. Process schematic diagrams of (a) the preparation of NWs by dynamic spin coating method, (b) the preparation of electrode arrays by lithography technology, and (c) the preparation of electrode arrays by shadow mask technology. (d) Schematic representation of electrical contacts realized by landing metallic needle probes on the NWs.

nature, while the memcapacitive element is essentially a resistance with a power consumption limit [53].

3.1. Working mechanism of memresistive nanowires

Characterized by resistive switching memory, memresistive nanowire is usually composed of active metal (core) and electrolyte materials (shell). The commonly used electrolyte materials are inorganic compounds such as Ag_2S, TiO_2, and NiO_2 besides of polymers like PVP. Memdevices with MIM structure have various working mechanisms depending on the different functional materials [54]. The memresistive junctions here rely on the principle of electrochemical redox reactions to work. At first, the metal on both sides of the junction is separated by an insulator in the middle, contributing to a high resistance state (off state). When a certain voltage is applied to the nanowires to generate an electrical potential difference between the metal Ag wires on both sides of the electrolyte layer in the junctions, on the one hand, the Ag wires at anode will be induced to undergo oxidation reaction to form Ag^+ ions; on the other hand, an electrical field from the anode to cathode will be generated in the electrolyte layer which further leads to the drift of Ag^+ ions at anode to cathode. As a result, the Ag^+ ions continuously obtain electrons at the cathode and are reduced into Ag nanoparticles which subsequently gather into nanoclusters and grow in different ways, finally forming Ag conductive filaments with different branch structures [55, 56]. The electrodes at both ends are connected through the filament to make the junctions reach a low resistance state (on state) from a high resistance state, which is called set process [57], as can be seen in figure 4(a). When the applied voltage is removed, the Ag^+ ions on the cathode side with much higher concentration than the anode side will spontaneously diffuse to the anode to reach the equilibrium state under the driving of the nanobattery effect including the minimization of interfacial energy and internal electro-dynamic potential, which in turn induces the spontaneous dissolution of conductive filament [58, 59]. Therefore, the junctions recover from the low resistance state to the initial high resistance state, reflecting the volatility of open current.

Depending on this mechanism, the memresistive junctions can be switched between high and low resistance states by controlling the externally applied bias voltage. The resistive switching properties have two cases, that is, unipolar resistive switch unrelated to voltage polarity and bipolar resistive switch related to voltage polarity [60, 61]. Because of the symmetrical junction structure, nanowires exhibit unipolar resistive switching behavior. Additionally, the high and low resistance states can be maintained for a certain period of time, which is similar to the memory characteristic of human brain. This characteristic of memresistive nanowires is thus called unipolar and volatile resistive switching memory characteristic, which can be observed through current–voltage (I–V) curves, as shown in figure 4(b).

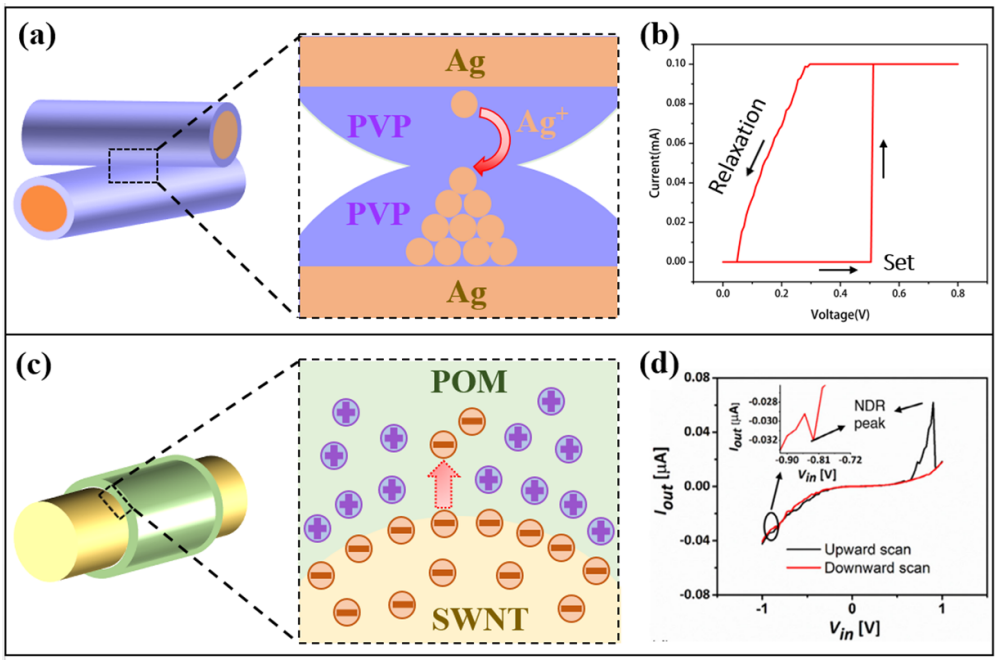

Figure 4. (a) Schematic representation of the memresistive mechanism in a single NW cross-point junction. (b) DC *I*–*V* curve of the conductive path with cascaded memresistive junctions in the NWs. (c) Schematic representation of the memcapacitive mechanism in a single NW cross-point junction. (d) Current trace (I_{out}) over cyclic voltage sweeps (V_{in}) with upward (black line) and downward (red line) scan direction, and the inset shows the magnified downward bias black encircled region with a similar NDR peak. Reproduced from [49]. CC BY 4.0.

3.2. Working mechanism of memcapacitive nanowires

The working mechanism of memcapacitive nanowires is based on the redox reaction of molecules which results in the charging and discharging behavior of the junction capacitor, and then affects the conductance and causes the conductance switching behavior [62]. POM molecules such as PMo_{12} ($H_3PMo_{12}O_{40}$), on the one hand, is able to store 24 electrons and induce the change of the molecular structure, so it has the reversible multi-electron redox characteristic [63]. When a heterogeneous molecular capacitive junction is formed between SWNT and POM, POM molecules can absorb electrons (charging) from the coated SWNT to undergo reduction reaction, thus reducing the current flowing through SWNT. Meanwhile, a large amount of charge stored in POM molecules will cause a large electrical potential difference in the junction, leading to a transition from low to high conductance state. On the contrary, when a large number of electrons are gathered, POM molecules can also release extra electrons (discharging), resulting in oxidation reaction. As a result, the current flowing through SWNT increases, contributing to a transition from high to low conductance [48], as shown in figure 4(c). On the other hand, POM molecules absorbed on SWNT produce negative differential resistance (NDR), which is closely related to the multiple redox reactions in memcapacitive junctions [64]. However, the physical principle of NDR phenomenon has not been fully understood up to date. The NDR effect of SWNT/POM nanowires can be observed from the DC *I*–*V* characteristic curve (figure 4(d)), that is, the current decreases with the increase of applied voltage [49].

4. Dynamic characteristics of NWs

Regarded as a complex network formed by a large number of randomly connected memresistive or memcapacitive junctions, the self-assembled NWs have a disordered structure which is difficult to be prepared by traditional top-down techniques and gives rise to unique dynamics. The dynamic characteristics of NWs is essentially the collective electrical behavior of these interacting junctions.

4.1. Dynamic characteristics related to network topologies

4.1.1. Small-worldness and modularity. The self-assembled NW (figure 5(a)) with a highly similar topological structure to biological neural network (figure 5(b)), is a kind of network structure between ordered grid-like network and random network. It shows small word connectivity, namely a network connection structure combining local clustering and short path length, and modularity which reflects that the network is isolated into different sparsely connected modules [65, 66]. And this connection structure is believed to have a close relationship with the network functions such as cognitive function and information transmission capability [67–70]. Recently, Milcano *et al* studied the relationship between the structure and function of NWs using the graph theory method. By observing the dynamic evolution process of the information flow in the memresistive NW, they proved that the critical behavior of the network under the external stimulus would lead to the formation of a self-selected conductive path, thus maximizing the information flow and minimizing the

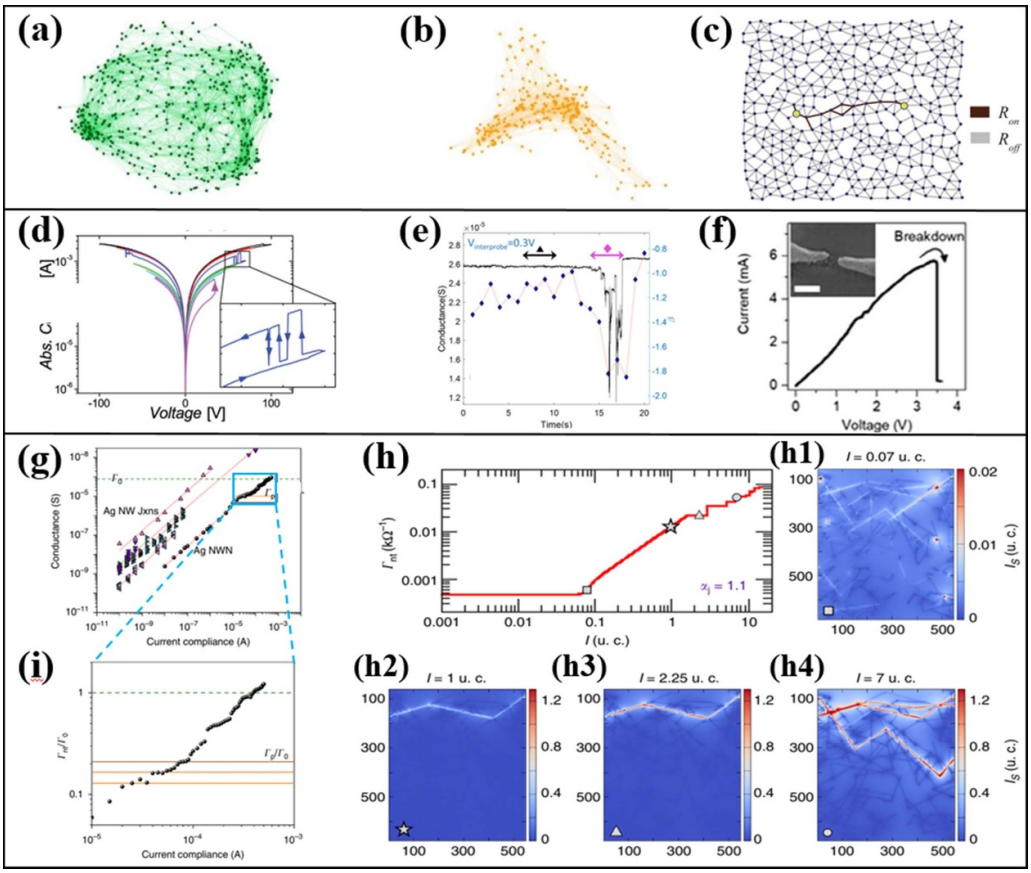

Figure 5. (a) Graphical representations of (a) NWs and (b) biological neural network. Reproduced from [66]. CC BY 4.0. (c) Solutions of the shortest-path optimization problem by a random memresistive network. Reprinted figure with permission from [75], Copyright (2013) by the American Physical Society. (d) Adaptive reconfiguration of the current paths under high stress in large networks. Reproduced from [77] with permission from the Royal Society of Chemistry. (e) Conductance time series with small fluctuations of Ag/PVP NWs. Reproduced from [72]. CC BY 4.0. (f) Electrical breakdown of a single nanowire showing a sudden drop in current. The inset exhibits the SEM image of a breakdown-induced nanogap. Reproduced from [79]. CC BY 4.0. (g) Conductance plotted against the current compliance of Ag nanowire junctions and NWs for numerous nanowire systems. (i) Zoom-in at the high current compliance range of the Γ_{nt} taken from panel (g) and divided by Γ_0. (h) The network conductance versus current curve for the Ag NWs, and (h1)–(h4) current maps calculated over different wire segment (I_s), which are distinguished by the symbols: square (transient growth), star (power-law), triangle and circle (both set in the post-power-law regime). Reproduced from [76]. CC BY 4.0.

information transmission distance, helping to process timing input signals [71].

4.1.2. WTA characteristic. When a voltage greater than the threshold voltage for network activation is applied, the network will be activated by forming a conductive path connecting the electrodes at both terminals. The conductive path is composed of a large number of cascaded junctions and metal wires, whose formation is marked by the collective transformation of cascaded junctions from a high to low resistance state [72, 73]. In theory, there are many different conductive paths can be formed between the two electrodes. However, the formation of conductive paths in the NW has the WTA property, that is, once the optimal transmission path is formed under a certain voltage, other paths will be inhibited. And the optimal transmission path is generally the path with the smallest resistance and shortest distance [74], as can be seen in figure 5(c). Thanks to the memory ability of nanowire junctions, the network is able to self-assemble to form WTA conductive path according to its own structural features, with the driving force coming from the reduction of network entropy [73, 75]. The network circuits with WTA characteristic are proven to have universal digital and analog computing power [76].

4.1.3. Adaptive reconfiguration characteristic. Due to the introduction of resistive switch junctions, the NWs have the programmable properties which cannot be realized by traditional materials. The network with the ability of dynamically redistributing the distribution of switch junctions, is with fault tolerance, adaptive properties, and structural plasticity. The large networks with inherent redundancy of junctions are enabled to spontaneously program and reconstruct conductive paths by activating the alternative local paths or reactivating the junctions restoring the initial state. In figure 5(d), the conductance of networks in the enlarged I–V curve suddenly drops, but then reaches a new higher conductance level a few seconds later. Under

electrical stimulation, this dynamic reconfigurable property is a prominent feature of NWs and continues until a stable conductive path is established [77]. Diaz-Alvarez *et al* also found that the conductance of the stable NWs would fluctuate irregularly after a large disturbance, but would soon automatically returns to the new stable state [72], as shown in figure 5(e). In addition, Batra *et al* found that when nanowires break resulting from joule thermal and electrical breakdown, needle-like nanowire gaps are generated and the conductance suddenly drops [78]. Interestingly, there are new conductive filaments reformed under the impact of electro-migration driven by electrical field and bipolar electrode effects, leading to electrical connection in the nanogaps, and thus exhibiting excellent structural plasticity [79], as shown in figure 5(f).

4.1.4. Power law scaling property. The conductance (Γ) and compliance current (I_c) of a single junction and the whole network interconnected by cascaded junctions show a power law scaling behavior: $\Gamma = AI_c^{\alpha}$, α is the scaling factor, and A is a constant, as shown in figure 5(g). This indicates that the growth of conductive filaments in the single nanowire junctions is similar to the formation of current paths in the networks. Under the case of quantum conductance (Γ_0), the network conductance (Γ_{nt}) curves contain many conductance platforms, at each of which the Γ_{nt} is stable within a certain input current range and the network connection will not be greatly affected (figure 5(i)). In figure 5(h), further simulation results show that the appearance of conductance platform is closely related to the formation of WTA conductance path [73, 74]. With the increase of I_c, the Γ_{nt} exhibits four phases: ① OFF (OFF-threshold) phase (figure 5(h1)), where all junctions are in the OFF state, and no conductive path is formed. ② TG (transient growth) phase (figure 5(h2)), when the Γ_{nt} exceeds a certain threshold, a current path begins to form. Theoretically, the conductive paths can grow in a variety of ways. But the network chooses the WTA path which is easiest for current conduction and has the lowest forming energy, and then the network temporarily changes into ohm state, representing the appearance of the first conductance platform. ③ PL (power law) phase (figure 5(h3)), where the WTA path gradually becomes stable, and the Γ_{nt} remains unchanged within a certain current range. ④ PPL (post-PL) phase (figure 5(h4)), multiple WTA paths are gradually generated with the further increase of current.

4.2. Dynamic characteristics related to RC performance

The dynamics of network topological structure and connectivity endow NWs with rich time-varying information processing dynamics in neuromorphic computing [80]. Here, we emphasize on the emergent dynamics related to RC.

4.2.1. Short-term memory property. The short memory property also named fading memory and echo state characteristic refers to the fact that the state of NWs-based reservoir manifests as decay behavior and is not only linked with the current input signals but also the recent-past ones, while has nothing to do with the distant-past ones [81]. Specifically, when disturbed by an input stream, the reservoir states exhibit a notable change, and eventually relax to its initial level after a period of being unperturbed. Hence, it is beneficial to guarantee the similar change and final level after degradation of the internal reservoir states when suffering from the similar input stimulation. Besides, the implementation of short-term memory is considered to be determined by the weight matrix initialization [82].

In general, it is believed that this property stems from the inherent volatile state linked to the formation and spontaneous dissolution of unstable conductive filaments in junctions of NWs-based memresistive reservoir. Through mapping the NWs to a weighted grid diagram, Daniel and collaborators simulated the spatiotemporal evolution of the conductive path formation and following dissolution, and found the process is a history-dependent behavior, which demonstrates the short-term memory property from the simulated point of view [40]. Experimentally, Li *et al* observed the formation process of conductive paths taking advantage of lock-in thermography (LIT) technique (figure 6(a)), and found that part of the conductive paths can be reused when the electrode position applied with voltage was changed sequentially (figures 6(b)–(e)), which also confirmed the short-term memory capacity of the reservoir [83]. Moreover, the relaxation characteristic curve can be adjusted by changing the input pulse parameters such as pulse amplitude, width, and frequency, which also exists in other devices [84]. In practice, this property is of great importance to tackle the tasks concluding time series connection.

4.2.2. Nonlinearity characteristic. The nonlinearity refers to the ability of projecting the inputs to a high-dimensional space, of which, the degree of nonlinearity is generally closely related to that of complexity in a RC system, allowing the reservoir to transform from a static state (low complexity) to a chaotic regime (high complexity) [85, 86]. A RC system whose accuracy depends on the degree of complexity, performs best close to its chaotic state [104, 24, 87]. In addition, the stability of nonlinearity can be quantitatively evaluated by a local Lyapunov exponent which is used to judge the sensitivity of a RC system to initial value, that is, chaos phenomenon [88]. Specially, the negative exponent indicates that the system is stable, while the positive exponent means that the system is sensitive to the initial value and has chaotic behavior. The memory capacity of reservoir possesses a negative correlation with the system stability, which is maximized at the edge of chaos and then decreases quickly when the system becomes chaotic [89, 90]. Thereby, it is of great importance to regulate the nonlinearity to drive RC system to the edge of chaos for receiving best performance. This property is crucial to realize the transformation from linear indivisibility to divisibility of the inputs.

When a DC voltage is applied to the NWs-based reservoir, the response of the current to the voltage is nonlinear, as shown in the *I*–*V* curves with a notable hysteresis window, which can be ascribed to the relatively slow migration of ions at memresistive junctions in response to the voltage sweep [91].

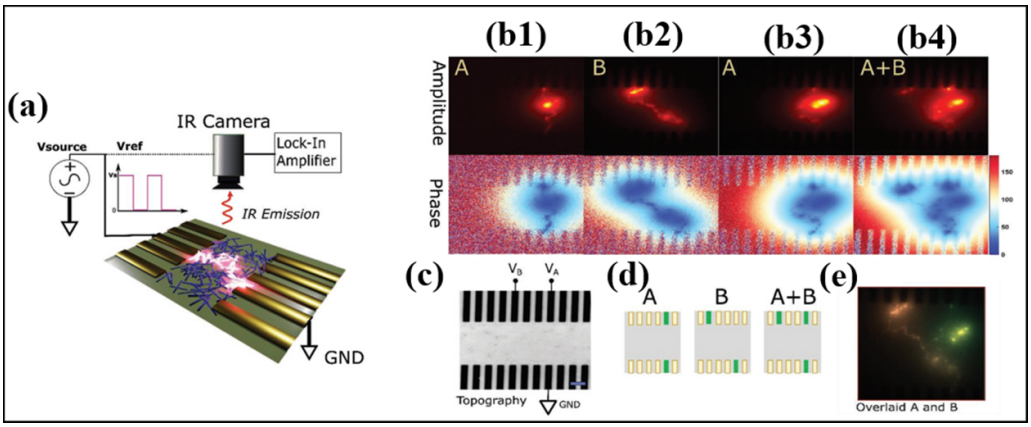

Figure 6. (a) Illustration of measurement scheme during operation of LIT technique, in which power dissipation in the Ag/TiO_2 NWs as a result of Joule heating can be sensitively imaged through infrared (IR) radiation. (b) Lock-in amplitude (top) and phase (bottom) images taken sequentially on the network as two different electrodes. (c) Optical micrograph image of the network and multi-electrodes. (d) Scheme of opened electrodes in different configurations. (e) Overlay of lock-in amplitude images of (b2) and (b3), where B and A configurations are probed separately. [83] John Wiley & Sons. [© 2020 Wiley-VCH GmbH].

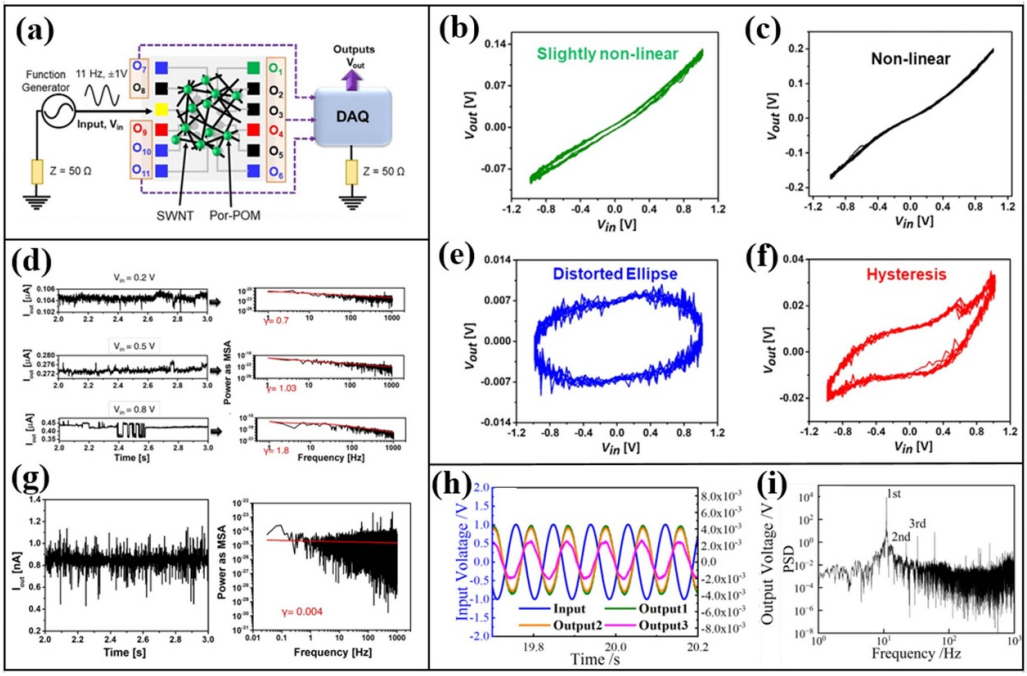

Figure 7. (a) Full circuit measurement scheme of nanowire reservoir device where the function generator is used to provide input signal to the NWs and all outputs are taken from the DAQ (data acquisition) system. (b) Slightly nonlinear Lissajous plot (LP) with no phase delay shows a proportional change in output voltage (V_{out}) amplitude relative to the input voltage (V_{in}) representative of resistive pathways. (c) The nonlinear LP represents the charge–discharge phenomena occurring but with signals in phase with the input. (d) The elliptical and (e) the hysteresis with NDR like fluctuations show phase delays corresponding to the complex capacitive network pathways. Current output response and corresponding PSD plot with different scaling factor (γ) obtained from FFT for (d) different input bias and (g) 0 V input DC bias. Reproduced from [49]. CC BY 4.0. (h) Input voltage-time curves and (i) corresponding PSD diagram for a random network reservoir device made from Ag/Ag_2Se nanowires responding to an input signal. Reproduced from [45]. CC BY 4.0.

In addition, when an AC voltage is applied to the NW-based reservoir, Tanaka *et al* used the circuit scheme (figure 7(a)) to collect the outputs on different electrodes via Lissajous sampling principle [92, 93], and found that the phase and frequency generated various degree of change compared with the input signal, which demonstrates that NWs-based reservoir with intrinsic nonlinearity can perform a nonlinear conversion for inputs, as shown in figures 7(b)–(f).

4.2.3. Separation property. The separation property describes the ability to distinguish and divide input signals including different feature information from each other and divide them to different categories, which ensures markedly distinct responses in regard of reservoir states for various time-dependent input signals [82]. Empirically, the analysis of the degree of separation can be conducted taking advantage of the rank of reservoir internal weight matrix consisted

of state vectors, which is defined as the number of linearly independent reservoir state vector [10, 94]. Banerjee *et al* carried out fast Fourier transformation (FFT) on the output information of SWNT/Por-POM NWs-based reservoir under different input bias (figures 7(d) and (g)), and used the $1/f^{\gamma}$ (f is the frequency) power-law scaling formula to fit the transformed power spectral density (PSD)-f curves and obtained different γ values, which indicates that different input signals can be distinguished. The NW is thus proven to have the separation property [49].

4.2.4. Approximation property. The approximation property is the ability to group similar input signals into the same class, and requires to be insensitive to small intrinsic fluctuations such as noise simultaneously. This property is not only closely related to the number of effective reservoir states, but also essential to the characteristics of specific applications, which is linked with the complexity of solvable tasks and computational accuracy [95, 96]. However, there is no general rules to quantify the degree of approximation of the same class inputs, which is similar to the case of evaluating separation property [82]. Due to the operation mechanism based on the stochastic formation and spontaneous dissolution of local conductive filament, the outputs of reservoir with memresistive junctions usually have a big cycle-to-cycle variation, causing poor separation and approximation properties.

4.2.5. High-dimensional property. High-dimensional property means that the reservoir has a sufficient degree of complexity to ensure a high-dimensional feature space for feature extraction. Deriving from interactions of abundant nonlinear junctions amongst the interconnected complex networks, this property is important for feature extraction of input signals and helps to separate originally indivisible inputs in classification tasks, thus contributing to achieve multiple classifications with high accuracy. The dimension of feature space is highly connected with the number of effective reservoir states or rather the independent output signals obtained from the reservoir. One effective state can represent a feature. The higher the degree of dimensions in the projected domain is, the more successful the separation is. Kotooka *et al* acquired the curve of PSD as a function of frequency via FFT analysis of the output signals (figures 7(h) and (i)), and observed higher harmonic (2nd and 3rd) apart from fundamental frequency signal (1st), indicating that the reservoir exhibits high-dimensional mapping [45].

5. Applications of NWs-based RC

Owing to rich dynamic characteristics, previous studies have demonstrated the feasibility of NWs to be used as a platform of RC to solve some time series problems [97–101]. For different inputs which correspond to different tasks, it is important to conduct the training of weights through supervised learning. Only with effective training can NWs-based RC provide a high computational accuracy.

5.1. Training methods

For different tasks corresponding to different $u(t)$, effective training of W_{out} is highly important. The aim of training is to implement the minimization of the loss function which is defined as the difference between the output signal ($y(t)$) and the target signal. At present, there are two dominating linear regression algorithms for W_{out} training, namely the least square method and ridge regression method, which can be expressed by the following formulas respectively:

$$W_{\text{out}} = \left(\mathrm{X}^{\mathrm{T}}\mathrm{X}\right)^{-1}\mathrm{X}^{\mathrm{T}}\mathrm{Y} \tag{7}$$

$$W_{\text{out}} = \left(\mathrm{X}^{\mathrm{T}}\mathrm{X} + k\mathrm{I}\right)^{-1}\mathrm{X}^{\mathrm{T}}\mathrm{Y} \tag{8}$$

where X, Y, I, and k are reservoir state matrix, target matrix, identity matrix, and hyper parameter, respectively [33, 102]. The main difference of ridge regression algorithm in the calculation method is artificially adding a non-negative factor k to the main diagonal element of the independent variable matrix compared with the least square method, which enables it to be used for the training of high-order target signals rather than simple periodic signals.

5.2. Neuromorphic applications

After sufficient and effective training, NWs-based RC systems with an optimized W_{out} can perform some neuromorphic computing tasks which can be divided to three categories: recognition, classification, and prediction tasks. For example, Milano *et al* built up an in-materio RC system with a fully memresistive architecture in which the reservoir consists of Ag/PVP self-organizing NWs and the read-out layer is made of Ta/TaO_x cross-bar array, they successfully use this RC system to implement Mackey–Glass time series prediction task with an accuracy of ∼90.6% which can be further improved with multiple reads during the computation [40]. Kotooka *et al* fabricated a new material-based reservoir device using Ag/Ag_2Se nanowire random networks for the purpose that the Ag_2Se nanowires have a better thermal stability than traditional Ag_2S nanowires. Based on as-constructed RC system, the voice identification and classification are carried out utilizing the free-spoken digit data as shown in figure 8(a). The voice of different speakers can be recognized and classified with an accuracy above 80% for all speakers [45], as shown in figures 8(b) and (c). Besides, Banerjee *et al* also introduced a physical RC platform comprised of SWNT/Por-POM complex-based recurrent NWs. The RC platform can realize object classification task which is demonstrated using the Toyota human support robot (HSR) tactile sensory input data. The Toyota HSR could grasp given objects according to the change in the gripper angle as a function of the applied forces collected by the force-torque sensor (figures 8(d) and (e)) [49]. Other than these tasks, NWs-based RC systems can also address other tasks like waveform generation tasks. Kotooka *et al* used Ag/Ag_2Se NWs-based RC system to generate the cosine waveform and achieved a high accuracy (∼99%) [45], as shown in figures 8(f) and (g). More recently, Daniels *et al* investigated the effect of

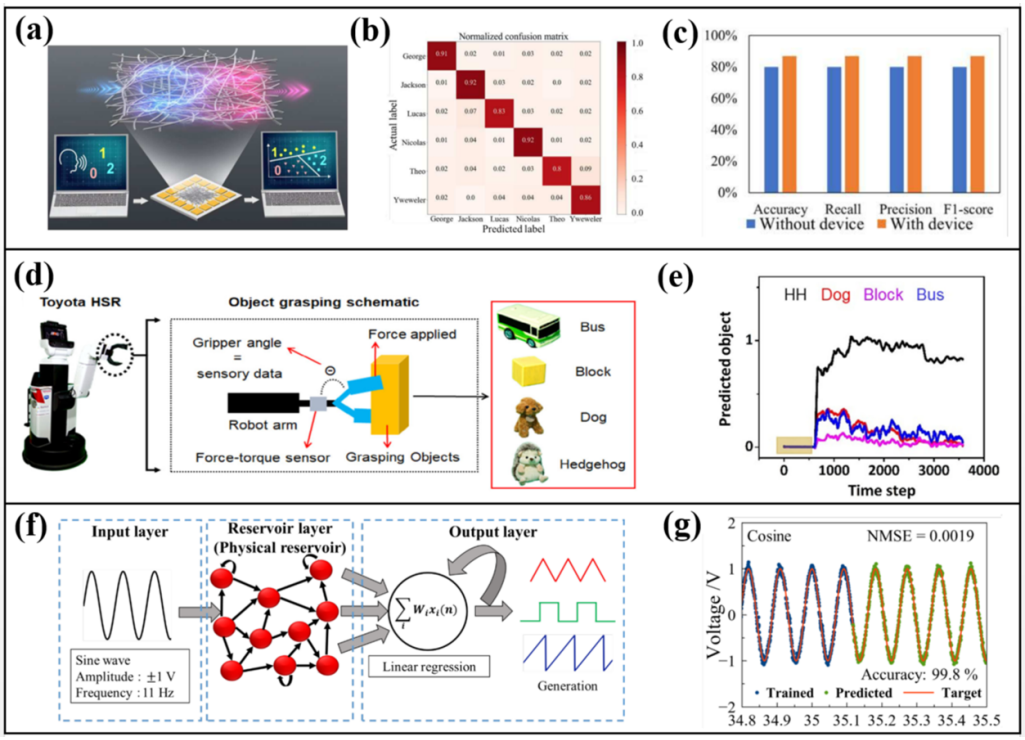

Figure 8. (a) Schematic of voice classification procedure. (b) Confusion matrix and (c) Classification scores of classifying different speakers with the Ag_2Se reservoir device. Reproduced from [45]. CC BY 4.0. (d) The HSR (left) with a schematic of the arm (middle) connected to the gripper via force-torque gathers tactile data from the change in the gripper angle and grasping force applied to objects (right) in the red box. (e) The predicted classification result of supervised binary object classification with SWNT/Por-POM reservoir. Reproduced from [49]. CC BY 4.0. (f) Procedure for waveform-generation task. (g) Results of cosine waveform generation tasks at room temperature. NMSE is an abbreviation for 'normalized mean square error'. Reproduced from [45]. CC BY 4.0.

stacking of nanowires on RC performance via detailed simulations to compare the performance of perfectly 2D and quasi-3D (stacked) NWs in memory capacity and nonlinear transformation, and eventually found that the various networks have a strikingly similar performance in RC tasks even if they are with radically different topologies, but also show important differences for example that the quasi-3D networks are more resilient to changes in the input parameters which generalizes better to noisy training data [103].

6. Future perspectives

In conclusion, we systematically reviewed the recent developments of nanowire networks (NWs)-based reservoir computing (RC) covering the aspects of device preparation, operation mechanism, dynamic characteristics, and applications. The reservoir preparation methods including two cases with or without organic matter are reviewed. Two working mechanisms for nanowires are expounded amply from memristive and memcapacitive principles. Several key dynamic characteristics such as small-worldness, winner takes all (WTA), adaptive reconfiguration, power law scaling, nonlinearity, short-term memory, high dimensional, separation, and approximation properties are summarized. Furthermore, the training methods on the basis of the least square and ridge regression principles other than the neuromorphic applications in recognition, classification, and prediction tasks have been discussed.

Existing results suggest that the research of NWs-based RC is still in the early stages. In spite of some advances, there are many challenges remained to be solved for the next step. Firstly, the commonly used nanowires in reservoir contain organic matter, making it incompatible with traditional complementary metal-oxide-semiconductor transistor (CMOS) technology and inconvenient to prepare. As such, it is necessary to explore new material systems with good compatibility especially the memcapacitive materials and nanowires which have rarely been reported. Additionally, developing new materials with higher dynamic complexity is also essential to improve computing competence for complex tasks. Secondly, only a few nanowires have been successfully applied to RC systems presently, more attempts in hardware implementation of reservoirs with new nanowires should be made to facilitate the progress of RC. Thirdly, it is not exactly clear what the specific behavior of reservoir is, so the reservoir is also treated as a 'black box', but does not make the system any less reliable [104]. Although it seems that some tasks are also tackled without the capture of how the reservoir operates, only by thoroughly understanding the

working mechanism can we design reservoir better. Fourthly, the NWs-based reservoir can only handle some relatively simple benchmark tasks, thereby the more efforts should be paid to the realization of more complex tasks. Fifthly, for memristive reservoir, its cycle-to-cycle repeatability of the dynamic response for identical external stimulus is awfully poor owing to the stochastic generation process of local conductive paths in the junctions [105]. This adversely affects the separation and appropriation properties of reservoirs, which is one of the dominating reasons for dissatisfactory computing power. So attentions should be paid to take measures to control the variation of output response to achieve ideal computing results. Sixthly, the performance of RC systems hinges on dynamic properties. But there is no general rule on the quantification of dynamic properties which determine the computing performance of RC systems and of which the influence on the computing performance can only be evaluated via the final calculation accuracy. We reckon each property has its optimal range of action and it is critical to quantify the properties to establish the relationship between each characteristic and computing performance as well as the constraint relation among these properties, contributing to the design of reservoir device with expected performance and to the regulation of dynamic properties to adapt the requirements of different tasks. Seventhly, it is a consensus that the reservoir working at the edge of chaos has optimal performance, but how to use chaos theory to design appropriate parameters to make reservoir just at the edge of chaos remains to be clarified. Eighthly, the hardware implementation of NWs-based reservoirs usually employs analogue-digital hybrid method, where the dynamic reservoir layer is analogue and the readout layer is digital. Recently, Tang et.al and colleagues have reported a fully analogue memristor-based RC system and highlighted that the power consumption of the fully analogue approach which allows signals to be transmitted and processed without any conversion is far lower than the systems containing digital hardware [106, 107]. Therefore, the fully analogue hardware implantation deserves attentions and efforts in the realm of NWs-based RC. Finally, limited to the intrinsically slow speed of ionic migration in junctions, the possibilities of applying in substantially high input frequencies should be taken into account and evaluated. And more studies are needed on the encoding and decoding algorithm of the input information with a spatiotemporal nature [108]. We ought to be aware of the fact that the road ahead to the application of NWs-based RC to real life will be long despite the superior computing merits, which calls for continuous efforts in the future.

Acknowledgments

This work was financially supported by the National Key R&D Program of China (Grant No. 2020AAA0109005), the Strategy Priority Research Program of Chinese Academy of Sciences (Grant No. XDA0330100), the Beijing Municipal Science & Technology Commission Program of China (Grant No. Z201100004320004), and the China Association for Science and Technology (Grant No. 2019Q1NRC001).

Conflict of interest

The authors declare that they have no known competing financial interests or personal relationships that could have appeared to influence the work reported in this paper.

ORCID iD

Dashan Shang https://orcid.org/0000-0003-3573-8390

References

[1] Zhang W Q, Gao B, Tang J, Yao P, Yu S, Chang M F, Yoo H J, Qian H and Wu H Q 2020 Neuro-inspired computing chips *Nat. Electron.* **3** 371–82
[2] Tanaka K, Tokudome Y, Minami Y, Honda S, Nakajima T, Takei K and Nakajima K 2022 Self-organization of remote reservoirs: transferring computation to spatially distant locations *Adv. Intell. Syst.* **4** 2100166
[3] Zidan M A, Strachan J P and Lu W D 2018 The future of electronics based on memristive systems *Nat. Electron.* **1** 22–29
[4] Salahuddin S, Ni K and Datta S 2018 The era of hyper-scaling in electronics *Nat. Electron.* **1** 442–50
[5] Onen M, Emond N, Wang B M, Zhang D F, Frances M R, Li J, Yildiz B and Alamo J A 2022 Nanosecond protonic programmable resistors for analog deep learning *Science* **377** 539–43
[6] Tang J S *et al* 2019 Bridging biological and artificial neural networks with emerging neuromorphic devices: fundamentals, progress, and challenges *Adv. Mater.* **31** e1902761
[7] Duan Q X, Jing Z K, Zou X L, Wang Y H, Yang K, Zhang T, Wu S, Huang R and Yang Y C 2020 Spiking neurons with spatiotemporal dynamics and gain modulation for monolithically integrated memristive neural networks *Nat. Commun.* **11** 3399
[8] Ham D, Park H, Hwang S and Kim K 2021 Neuromorphic electronics based on copying and pasting the brain *Nat. Electron.* **4** 635–44
[9] Jaeger H 2001 *The "Echo State" Approach to Analysing and Training Recurrent Neural Networks with an Erratum Note* (Bonn: German National Research Center for Information Technology GMD Technical Report) vol 148 p 13
[10] Maass W, Natschlager T and Markarm H 2002 Real-time computing without stable states a new framework for neural computation based on perturbations *Neural Comput.* **14** 2531–60
[11] Tran D and Teuscher C 2021 Computational capacity of complex memcapacitive networks *ACM J. Emerg. Technol. Comput. Syst.* **17** 1–25
[12] Benjamin S, David V and Jan V C 2007 An overview of reservoir computing: theory, applications and implementations *Proc. 15th European Symp. on Artificial Neural Networks* pp 471–82
[13] Vlachas P R, Pathak J, Hunt B R, Sapsis T P, Girvan M, Ott E and Koumoutsakos P 2020 Backpropagation algorithms and reservoir computing in recurrent neural networks for the forecasting of complex spatiotemporal dynamics *Neural Netw.* **126** 191
[14] Appeltant L, Soriano M C, Sande V G, Danckaert J, Massar S, Dambre J, Schrauwen B, Mirasso C R and Fischer I 2011 Information processing using a single dynamical node as complex system *Nat. Commun.* **2** 468

[15] Penkovsky B 2017 Theory and modeling of complex nonlinear delay dynamics applied to neuromorphic computing *Doctoral Dissertation* Université Bourgogne Franche-Comté

[16] Gallicchio C and Micheli A 2022 Architectural richness in deep reservoir computing *Neural Comput. Appl.* 1–18

[17] Gallicchio C, Micheli A and Pedrelli L 2017 Deep reservoir computing: a critical experimental analysis *Neurocomputing* **268** 87–99

[18] Gauthier D J, Bollt E, Griffith A and Barbosa W A S 2021 Next generation reservoir computing *Nat. Commun.* **12** 5564

[19] Jaurigue L and Ludge K 2022 Connecting reservoir computing with statistical forecasting and deep neural networks *Nat. Commun.* **13** 227

[20] Jang Y H, Kim W, Kim J, Woo K S, Lee H J, Jeon J W, Shim S K, Han J and Hwang C S 2021 Time-varying data processing with nonvolatile memristor-based temporal kernel *Nat. Commun.* **12** 5727

[21] Zhong Y N, Tang J S, Li X Y, Gao B, Qian H and Wu H Q 2021 Dynamic memristor-based reservoir computing for high-efficiency temporal signal processing *Nat. Commun.* **12** 408

[22] Du C, Cai F X, Zidan M A, Ma W, Lee S H and Lu W D 2017 Reservoir computing using dynamic memristors for temporal information processing *Nat. Commun.* **8** 2204

[23] Moon J, Ma W, Shin J H, Cai F X, Du C, Lee S H and Lu W D 2019 Temporal data classification and forecasting using a memristor-based reservoir computing system *Nat. Electron.* **2** 480–7

[24] Nishioka D, Tsuchiya T, Namiki W, Takayanagi M, Imura M, Koide Y, Higuchi T and Terabe K 2022 Edge-of-chaos learning achieved by ion-electron-coupled dynamics in an ion-gating reservoir *Sci. Adv.* **8** eade1156

[25] Nako E, Toprasertpong K, Nakane R, Takenaka M and Takagi S 2022 Experimental demonstration of novel scheme of HZO/Si FeFET reservoir computing with parallel data processing for speech recognition *2022 IEEE Symp. on VLSI Technology and Circuits* pp 220–1

[26] Liu K Q, Zhang T, Dang B J, Bao L, Xu L Y, Cheng C D, Yang Z, Huang R and Yang Y C 2022 An optoelectronic synapse based on α-In_2Se_3 with controllable temporal dynamics for multimode and multiscale reservoir computing *Nat. Electron.* **5** 761–73

[27] Nako E, Toprasertpong K, Nakane R, Wang Z, Miyatake Y, Takenaka M and Takagi S 2020 Proposal and experimental demonstration of reservoir computing using $Hf_{0.5}Zr_{0.5}O_2$/Si FeFETs for neuromorphic applications *2020 IEEE Symp. on VLSI Technology and Circuits* pp 1–2

[28] Torrejon J *et al* 2017 Neuromorphic computing with nanoscale spintronic oscillators *Nature* **547** 428–31

[29] Prychynenko D, Sitte M, Litzius K, Krüger B, Bourianoff G, Kläui M, Sinova J and Everschor-Sitte K 2018 Magnetic skyrmion as a nonlinear resistive element: a potential building block for reservoir computing *Phys. Rev. Appl.* **9** 014034

[30] Vandoorne K, Mechet P, Van V T, Fiers M, Morthier G, Verstraeten D, Schrauwen B, Dambre J and Bienstman P 2014 Experimental demonstration of reservoir computing on a silicon photonics chip *Nat. Commun.* **5** 3541

[31] Van D S G, Brunner D and Soriano M C 2017 Advances in photonic reservoir computing *Nanophotonics* **6** 561–76

[32] Cucchi M *et al* 2021 Reservoir computing with biocompatible organic electrochemical networks for brain-inspired biosignal classification *Sci. Adv.* **7** eabh0693

[33] Usami Y *et al* 2021 In-materio reservoir computing in a sulfonated polyaniline network *Adv. Mater.* **33** e2102688

[34] Wakabayashi S, Arie T, Akita S, Nakajima K and Takei K 2022 A multitasking flexible sensor via reservoir computing *Adv. Mater.* **34** e2201663

[35] Kan S, Nakajima K, Takeshima Y, Asai T, Kuwahara Y and Akai-Kasaya M 2021 Simple reservoir computing capitalizing on the nonlinear response of materials: theory and physical implementations *Phys. Rev. Appl.* **15** 024030

[36] Sun W X *et al* 2022 3D reservoir computing with high area efficiency (5.12 TOPS/mm^2) implemented by 3D dynamic memristor array for temporal signal processing *2022 IEEE Symp. on VLSI Technology and Circuits* pp 222–3

[37] Yu J *et al* 2021 Energy efficient and robust reservoir computing system using ultrathin (3.5 nm) ferroelectric tunneling junctions for temporal data learning *2021 IEEE Symp. on VLSI Technology and Circuits* pp 1–2

[38] Ren K, Zhang W Y, Wang F, Guo Z Y and Shang D S 2022 Next-generation reservoir computing based on memristor array *Acta Phys. Sin.* **71** 140701

[39] Kaspar C, Ravoo B J, van der Wiel W G, Wegner S V and Pernice W H P 2021 The rise of intelligent matter *Nature* **594** 345–55

[40] Milano G, Pedretti G, Montano K, Ricci S, Hashemkhani S, Boarino L, Ielmini D and Ricciardi C 2022 In materia reservoir computing with a fully memristive architecture based on self-organizing nanowire networks *Nat. Mater.* **21** 195–202

[41] Kuncic Z and Nakayama T 2021 Neuromorphic nanowire networks: principles, progress and future prospects for neuro-inspired information processing *Adv. Phys.* X **6** 1894234

[42] Massey M K, Kotsialos A, Volpati D, Vissol-Gaudin E, Pearson C, Bowen L, Obara B, Zeze D A, Groves C and Petty M C 2016 Evolution of electronic circuits using carbon nanotube composites *Sci. Rep.* **6** 32197

[43] Lilak S, Woods W, Scharnhorst K, Dunham C, Teuscher C, Stieg A Z and Gimzewski J K 2021 Spoken digit classification by in-materio reservoir computing with neuromorphic atomic switch networks *Front. Nanotechnol.* **3** 675792

[44] Kundu M, Terabe K, Hasegawa T and Aono M 2006 Effect of sulfurization conditions and post-deposition annealing treatment on structural and electrical properties of silver sulfide films *J. Appl. Phys.* **99** 103501

[45] Kotooka T, Lilak S, Stieg A Z, Gimzewski J, Sugiyama N, Tanaka Y, Tamukoh H, Usami Y and Tanaka H 2021 Ag_2Se nanowire network as an effective in-materio reservoir computing device (https://doi.org/10.21203/rs.3.rs-322405/v1)

[46] Du H W, Wan T, Qu B, Cao F Y, Lin Q R, Chen N, Lin X and Chu D W 2017 Engineering silver nanowire networks: from transparent electrodes to resistive switching devices *ACS Appl. Mater. Interfaces* **9** 20762–70

[47] Wan T, Pan Y, Du H W, Qu B, Yi J and Chu D W 2018 Threshold switching induced by controllable fragmentation in silver nanowire networks *ACS Appl. Mater. Interfaces* **10** 2716–24

[48] Tanaka H, Akai-Kasaya M, Termeh Y A, Hong L, Fu L, Tamukoh H, Tanaka D, Asai T and Ogawa T 2018 A molecular neuromorphic network device consisting of single-walled carbon nanotubes complexed with polyoxometalate *Nat. Commun.* **9** 2693

[49] Banerjee D, Kotooka T, Azhari S, Usami Y, Ogawa T, Gimzewski J K, Tamukoh H and Tanaka H 2022 Emergence of in-materio intelligence from an incidental structure of a single-walled carbon nanotube–porphyrin polyoxometalate random network *Adv. Intell. Syst.* **4** 2100145

[50] Demis E C, Aguilera R, Sillin H O, Scharnhorst K, Sandouk E J, Aono M, Stieg A Z and Gimzewski J K 2015

Atomic switch networks-nanoarchitectonic design of a complex system for natural computing *Nanotechnology* **26** 204003
[51] Cultrera A *et al* 2019 Mapping the conductivity of graphene with electrical resistance tomography *Sci. Rep.* **9** 10655
[52] Milano G, Cultrera A, Bejtka K, De L N, Callegaro L, Ricciardi C and Boarino L 2020 Mapping time-dependent conductivity of metallic nanowire networks by electrical resistance tomography toward transparent conductive materials *ACS Appl. Nano Mater.* **3** 11987–97
[53] Wang Z R *et al* 2018 Capacitive neural network with neuro-transistors *Nat. Commun.* **9** 3208
[54] Zhu J D, Zhang T, Yang Y C and Huang R 2020 A comprehensive review on emerging artificial neuromorphic devices *Appl. Phys. Rev.* **7** 011312
[55] Yang Y C, Gao P, Li L Z, Pan X Q, Tappertzhofen S, Choi S, Waser R, Valov I and Lu W D 2014 Electrochemical dynamics of nanoscale metallic inclusions in dielectrics *Nat. Commun.* **5** 4232
[56] Lee J and Lu W D 2018 On-demand reconfiguration of nanomaterials: when electronics meets ionics *Adv. Mater.* **30** 1702770
[57] Waser R, Dittmann R, Staikov G and Szot K 2009 Redox-based resistive switching memories-nanoionic mechanisms, prospects, and challenges *Adv. Mater.* **21** 2632–63
[58] Valov I, Linn E, Tappertzhofen S, Schmelzer S, van den Hurk J, Lentz F and Waser R 2013 Nanobatteries in redox-based resistive switches require extension of memristor theory *Nat. Commun.* **4** 1771
[59] Wang Z R *et al* 2017 Memristors with diffusive dynamics as synaptic emulators for neuromorphic computing *Nat. Mater.* **16** 101–8
[60] Waser R and Aono M 2007 Nanoionics-based resistive switching memories *Nat. Mater.* **6** 833–40
[61] Ielmini D and Wong H S P 2018 In-memory computing with resistive switching devices *Nat. Electron.* **1** 333–43
[62] Schwarz F, Kastlunger G, Lissel F, Egler-Lucas C, Semenov S N, Venkatesan K, Berke H, Stadler R and Lortscher E 2016 Field-induced conductance switching by charge-state alternation in organometallic single-molecule junctions *Nat. Nanotechnol.* **11** 170–6
[63] Hong L, Tanaka H and Ogawa T 2013 Rectification direction inversion in a phosphododecamolybdic acid/single-walled carbon nanotube junction *J. Mater. Chem.* C **1** 1137–43
[64] Mahmoud S K, In K S and Mark A B 1996 Ordered array formation and negative differential resistance behavior of cation-exchanged heteropoly acids probed by scanning tunneling microscopy *J. Mater. Chem.* **100** 19577–81
[65] Pantone R D, Kendall J D and Nino J C 2018 Memristive nanowires exhibit small-world connectivity *Neural Netw.* **106** 144–51
[66] Loeffler A, Zhu R, Hochstetter J, Li M, Fu K, Diaz-Alvarez A, Nakayama T, Shine J M and Kuncic Z 2020 Topological properties of neuromorphic nanowire networks *Front. Neurosci.* **14** 184
[67] Bassett D S and Bullmore E 2006 Small-world brain networks *Neuroscientist* **12** 512–23
[68] Muldoon S F, Bridgeford E W and Bassett D S 2016 Small-world propensity and weighted brain networks *Sci. Rep.* **6** 22057
[69] Rodriguez N, Izquierdo E and Ahn Y Y 2019 Optimal modularity and memory capacity of neural reservoirs *Netw. Neurosci.* **3** 551–66
[70] Bertolero M A, Yeo B T and D'Esposito M 2015 The modular and integrative functional architecture of the human brain *Proc. Natl Acad. Sci.* **112** E6798–807
[71] Milano G, Miranda E and Ricciardi C 2022 Connectome of memristive nanowire networks through graph theory *Neural Netw.* **150** 137–48
[72] Diaz-Alvarez A, Higuchi R, Sanz-Leon P, Marcus I, Shingaya Y, Stieg A Z, Gimzewski J K, Kuncic Z and Nakayama T 2019 Emergent dynamics of neuromorphic nanowire networks *Sci. Rep.* **9** 14920
[73] O'Callaghan C, Rocha C G, Niosi F, Manning H G, Boland J J and Ferreira M S 2018 Collective capacitive and memristive responses in random nanowire networks: emergence of critical connectivity pathways *J. Appl. Phys.* **124** 152118
[74] Manning H G *et al* 2018 Emergence of winner-takes-all connectivity paths in random nanowire networks *Nat. Commun.* **9** 3219
[75] Pershin Y V and Di V M 2013 Self-organization and solution of shortest-path optimization problems with memristive networks *Phys. Rev.* E **88** 013305
[76] Maass W 2000 On the computational power of winner-take-all *Neural Comput.* **12** 2519–35
[77] Bellew A T, Bell A P, McCarthy E K, Fairfield J A and Boland J J 2014 Programmability of nanowire networks *Nanoscale* **6** 9632–9
[78] Batra N M, Syed A and Costa P 2019 Current-induced restructuring in bent silver nanowires *Nanoscale* **11** 3606–18
[79] Milano G, Pedretti G, Fretto M, Boarino L, Benfenati F, Ielmini D, Valov I and Ricciardi C 2020 Brain-inspired structural plasticity through reweighting and rewiring in multi-terminal self-organizing memristive nanowire networks *Adv. Intell. Syst.* **2** 2000096
[80] Zhu R, Hochstetter J, Loeffler A, Diaz-Alvarez A, Nakayama T, Lizier J T and Kuncic Z 2021 Information dynamics in neuromorphic nanowire networks *Sci. Rep.* **11** 13047
[81] Gouhei T, Yamane T, Heroux J B, Nakane R, Kanazawa N, Takeda S, Numata H, Nakano D and Hirose A 2019 Recent advances in physical reservoir computing: a review *Neural Netw.* **115** 100–23
[82] Tran D T 2019 Memcapacitive reservoir computing architectures *Doctoral Dissertation* Portland State University
[83] Li Q, Diaz-Alvarez A, Iguchi R, Hochstetter J, Loeffler A, Zhu R, Shingaya Y, Kuncic Z, Uchida K I and Nakayama T 2020 Dynamic electrical pathway tuning in neuromorphic nanowire networks *Adv. Funct. Mater.* **30** 2003679
[84] Wan Q, Rasetto M, Sharbati M T, Erickson J R, Velagala S R, Reilly M T, Li Y, Benosman R and Xiong F 2021 Low-voltage electrochemical Li_xWO_3 synapses with temporal dynamics for spiking neural networks *Adv. Intell. Syst.* **3** 2100021
[85] Yang K, Joshua Y J, Huang R and Yang Y C 2021 Nonlinearity in memristors for neuromorphic dynamic systems *Small Sci.* **2** 2100049
[86] Kumar S, Wang X, Strachan J P, Yang Y and Lu W D 2022 Dynamical memristors for higher-complexity neuromorphic computing *Nat. Rev. Mater.* **7** 575–91
[87] Hochstetter J, Zhu R, Loeffler A, Diaz-Alvarez A, Nakayama T and Kuncic Z 2021 Avalanches and edge-of-chaos learning in neuromorphic nanowire networks *Nat. Commun.* **12** 4008
[88] Verstraeten D, Schrauwen B, D'Haen M and Stroobandt D 2007 An experimental unification of reservoir computing methods *Neural Netw.* **20** 391–403
[89] Liu K Q, Dang B J, Zhang T, Yang Z, Bao L, Xu L Y, Cheng C D, Huang R and Yang Y C 2022 Multilayer reservoir computing based on ferroelectric α-In_2Se_3 for

hierarchical information processing *Adv. Mater.* **34** e2108826
[90] Gallicchio C, Micheli A and Silvestri L 2018 Local Lyapunov exponents of deep echo state networks *Neurocomputing* **298** 34–45
[91] Fu Y M, Li H, Huang L, Wei T, Hidayati F and Song A 2022 Sputtered electrolyte-gated transistor with modulated metaplasticity behaviors *Adv. Electron. Mater.* **8** 2200463
[92] Scharnhorst K S, Carbajal J P, Aguilera R C, Sandouk E J, Aono M, Stieg A Z and Gimzewski J K 2018 Atomic switch networks as complex adaptive systems *Jpn. J. Appl. Phys.* **57** 03ED02
[93] Hisham A H and Mohamad R A 2012 Geometrical and graphical representations analysis of lissajous figures in rotor dynamic system *IOSR J. Eng.* **2** 971–8
[94] Maass W 2011 Liquid state machines: motivation, theory, and applications *Computability in Context: Computation and Logic in the Real World* (London: Imperial College Press) pp 275–96
[95] Goudarzi A and Stefanovic D 2014 Towards a calculus of echo state networks *Proc. Comput. Sci.* **41** 176–81
[96] Rostami E N H 2015 Three recurrent neural echo state networks with clustered reservoirs for prediction of nonlinear and chaotic time series *Appl. Intell.* **43** 460–72
[97] Stieg A Z, Avizienis A V, Sillin H O, Martin-Olmos C, Aono M and Gimzewski J K 2012 Emergent criticality in complex turing B-type atomic switch networks *Adv. Mater.* **24** 286–93
[98] Sillin H O, Aguilera R, Shieh H H, Avizienis A V, Aono M, Stieg A Z and Gimzewski J K 2013 A theoretical and experimental study of neuromorphic atomic switch networks for reservoir computing *Nanotechnology* **24** 384004
[99] Stieg A Z, Avizienis A V, Sillin H O, Aguilera R, Shieh H H, Martin-Olmos C, Sandouk E J, Aono M and Gimzewski J K 2014 Self-organization and emergence of dynamical structures in neuromorphic atomic switch networks *Memristor Networks* (Switzerland: Springer International Publishing) pp 173–209
[100] Stieg A Z, Avizienis A V, Sillin H O, Martin-Olmos C, Lam M L, Aono M and Gimzewski J K 2013 Self-organized atomic switch networks *Jpn. J. Appl. Phys.* **53** 01AA02
[101] Demis E C, Aguilera R, Scharnhorst K, Aono M, Stieg A Z and Gimzewski J K 2016 Nanoarchitectonic atomic switch networks for unconventional computing *Jpn. J. Appl. Phys.* **55** 1102B2
[102] Kan S, Nakajima K, Asai T and Akai-Kasaya M 2022 Physical implementation of reservoir computing through electrochemical reaction *Adv. Sci.* **9** e2104076
[103] Daniels R K, Mallinson J B, Heywood Z E, Bones P J, Arnold M D and Brown S A 2022 Reservoir computing with 3D nanowire networks *Neural Netw.* **154** 122–30
[104] Petrauskas L, Cucchi M, Grüner C, Ellinger F, Leo K, Matthus C and Kleemann H 2021 Nonlinear behavior of dendritic polymer networks for reservoir computing *Adv. Electron. Mater.* **8** 2100330
[105] Ye F, Kiani F, Huang Y and Xia Q F 2022 Diffusive memristors with uniform and tunable relaxation time for spike generation in event-based pattern recognition *Adv. Mater.* 2204778
[106] Zhong Y N *et al* 2022 A memristor-based analogue reservoir computing system for real-time and power-efficient signal processing *Nat. Electron.* **5** 672–81
[107] Editorial 2022 Reservoir computing with memristors *Nat. Electron.* **5** 623
[108] Xia Q F, Yang J J and Midya R 2022 The secret order of disorder *Nat. Mater.* **21** 132–42